

High Resolution Crystal Structures of the Deoxy, Oxy, and Aquomet Forms of Cobalt Myoglobin*

(Received for publication, June 14, 1996)

Eric Allen Brucker, John S. Olson, and George N. Phillips, Jr.‡

From the Department of Biochemistry and Cell Biology, Rice University, Houston, Texas 77005-1892

Yi Dou and Masao Ikeda-Saito

From the Department of Physiology and Biophysics, Case Western Reserve University School of Medicine, Cleveland, Ohio 44106-4970

The structures of the deoxy, oxy, and aquomet forms of native sperm whale myoglobin reconstituted with cobalt protoporphyrin IX have been determined by x-ray crystallography. As expected, cobalt myoglobin closely resembles native iron myoglobin in overall structure, especially in their respective aquomet forms. In the cobalt oxymyoglobin structure, the N_ε of distal histidine 64 lies within hydrogen bonding distance to both the oxygen atom directly bonded to the cobalt and the terminal oxygen atom, in agreement with previous EPR and resonance Raman studies. The metal atom in cobaltous myoglobin does show a small 0.06-Å out-of-porphyrin plane displacement when moving from the oxy to deoxy state. In the case of the native iron-containing myoglobin, the oxy to deoxy transition results in a larger 0.16-Å displacement of the metal farther out of the porphyrin plane, attributed to an increase in spin from S = 0 to S = 2. The small displacement in cobalt myoglobin is due to a change in coordination geometry, not spin state (S = 1/2 for both cobalt deoxy- and oxymyoglobin). The small out-of-porphyrin plane movement of cobalt which accompanies deoxygenation of myoglobin also occurs in cobalt hemoglobin and serves to explain why cooperativity, although reduced, is still preserved when iron is replaced by cobalt in human hemoglobin.

Cobalt myoglobin and cobalt hemoglobin, in which the heme prosthetic group (iron protoporphyrin IX) is replaced by cobalt protoporphyrin IX, are capable of reversible oxygen binding with affinities 50 to 100 times weaker than those of the native iron counterparts (1, 2). Cobalt myoglobins and hemoglobins have provided information about the electronic structure and stereochemistry of the bound oxygen molecule and the ligand-binding sites of myoglobins and hemoglobins through spectro-

scopic investigations. The EPR and resonance Raman spectroscopic features associated with the dioxygen complex of cobaltous myoglobin are altered in deuterated buffers, suggesting formation of a hydrogen bond between the bound oxygen and the distal histidine residue (3–5). The proposed hydrogen bond is supported by EPR studies on recombinant myoglobin mutants (6, 7). These interpretations, however, rely on an assumption of identical oxygen binding geometry in cobalt and native myoglobins and quantitative analyses of spectroscopic properties have been hampered by the lack of a high resolution crystal structure.

The cobaltous atom is low spin ($3d^7$, $S = 1/2$) both in oxy and deoxy forms. This is different from ferrous native myoglobins and hemoglobins where the electronic structure of the heme iron changes from ferrous high spin ($3d^6$, $S = 2$) to low spin states ($S = 0$) upon oxygenation. In the absence of the spin state changes associated with oxygenation of cobalt(II) globins no movement of the metal relative to the mean porphyrin plane would be predicted (8). Metal displacement from the porphyrin plane was proposed as a major contribution of the multiphasic kinetics of picosecond geminate ligand rebinding, as the displacement makes the metal less accessible to the ligand (9). A recent study has revealed the presence of similar multiphasic picosecond reactions of ligand rebinding to cobalt myoglobin (10), suggesting that either the cobalt atom does move out of the porphyrin plane or that the above explanation for the multiphasic kinetics is incorrect.

Knowledge of changes in the structure of the heme pocket is fundamental to our understanding of the mechanism of heme protein reactivity. Therefore it is essential to determine the structures of both liganded and unliganded forms. In addition to the proven utility of cobalt myoglobins and hemoglobins in spectroscopic investigations of their oxygen binding, cobalt substitution appears likely to prove useful in studying the effect of mutations on ligand binding kinetics (10, 11). However, until this work, structural information on cobalt myoglobins has been incomplete. A difference Fourier analysis of the cobalt deoxymyoglobin crystal structure at 2.5-Å resolution has been reported (12). Unfortunately, the structure was not refined and the experiment was done on cobalt mesoporphyrin myoglobin, in which the vinyl groups of protoporphyrin IX were replaced by ethyl groups. Preliminary results of the crystal structure of cobalt oxymyoglobin have also been reported (13), but the refinement was not completed. The oxidized form of cobalt myoglobin has been proposed to have a structure different from that of ferric myoglobin (14), but the cobaltic structure has not been previously reported.

To obtain more definitive interpretation of the spectroscopic and kinetic properties of cobalt myoglobin, we have determined

* This work was supported by United States National Institutes of Health Grants AR40252 (to G. N. P.), GM35649/HL47020 (to J. S. O.), GM51588 (to M. I. S.), and Postdoctoral Fellowship AR08355 (to E. A. B.), State of Texas Advanced Technology Program Grant 003604-025 (to G. N. P. and J. S. O.), Robert A. Welch Foundation Grants C-1142 (to G. N. P.) and C-612 (to J. S. O.), and the W. M. Keck Center for Computational Biology. The costs of publication of this article were defrayed in part by the payment of page charges. This article must therefore be hereby marked "advertisement" in accordance with 18 U.S.C. Section 1734 solely to indicate this fact.

The atomic coordinates and structure factors (codes 1YOG, 1YOH, 1YOI, and 2MBW) have been deposited in the Protein Data Bank, Brookhaven National Laboratory, Upton, NY.

‡ To whom correspondence should be addressed: Dept. of Biochemistry and Cell Biology, Rice University, 6100 South Main St., Houston, TX 77005-1892. Tel.: 713-527-4910; Fax: 713-285-5154; E-mail: georgep@rice.edu.

TABLE I
Selected cobalt myoglobin crystallographic data

	Deoxy	Oxy	Met
Unique reflections	12618	12355	11644
Resolution (Å)	1.65	1.65	1.65
Completeness (%)	81.1	78.8	74.5
<i>R</i> -merge (%)	10.1	4.3	3.8
Space group	P2 ₁	P2 ₁	P2 ₁
Unit cell			
<i>a</i> (Å)	64.71	64.68	64.53
<i>b</i> (Å)	30.78	30.92	30.95
<i>c</i> (Å)	34.87	34.91	34.89
β (°)	106.1	105.8	105.8
<i>R</i> cryst (%)	18.1	16.2	16.4
RMS deviation			
Bonds (Å)	0.02	0.02	0.02
Angles (°)	1.74	1.73	1.78
Dihedrals (°)	19.6	19.9	20.0
Impropers (°)	1.82	1.92	1.89

the high resolution crystal structures of the deoxy, oxy, and aquomet forms of sperm whale cobalt myoglobin. The results have been compared in detail to the corresponding structures of the native iron-containing protein.

MATERIALS AND METHODS

Crystallization—Preparation of the cobalt(II) protoporphyrin IX reconstituted sperm whale apomyoglobin protein has been described earlier (6, 14). Crystals were grown by the batch method (one part 60 mg ml⁻¹ protein, $\epsilon = 7.78$ ml mg⁻¹ cm⁻¹ at 425 nm, in unbuffered deionized H₂O mixed with three parts saturated aqueous (NH₄)₂SO₄) in a temperature controlled environment (17 °C). They were mounted in sealed quartz capillary tubes prior to data collection.

Data Collection and Structure Determination—The crystals were all monoclinic, space group P2₁, as originally solved by Kendrew (15). A single data set for each reported structure was collected at room temperature using a Rigaku Raxis IIC imaging plate system and copper K α radiation from a Siemens rotating anode operated at 50 mV and 90 mA.

Deoxy Cobalt Myoglobin—The crystal was brought into an anaerobic glove box and reduced overnight in a sodium dithionite/mother liquor solution. Then, the crystal was mounted and sealed in the quartz capillary before removal from the oxygen-free atmosphere. The unit cell dimensions were $a = 64.71$ Å, $b = 30.78$ Å, $c = 34.87$ Å, and $\beta = 106.1^\circ$. A total of 62,314 measured reflections from 119 images ($\Delta\omega = 1.5^\circ$) were reduced to 12,618 unique intensities (5.0 to 1.65 Å) with an *R*-merge of 10.1% for all data to a resolution of 1.65 Å (81.1% complete) using the DENZO software package (see Table I).

Oxy Cobalt Myoglobin—The crystal was reduced in a sodium dithionite/mother liquor solution overnight. Then, it was removed from the reducing solution and placed in a vial containing buffer equilibrated with one atmosphere of dioxygen for 1 h immediately prior to data collection. The unit cell dimensions were $a = 64.68$ Å, $b = 30.92$ Å, $c = 34.91$ Å, and $\beta = 105.8^\circ$. A total of 46,278 measured reflections from 120 images ($\Delta\omega = 1.5^\circ$) were reduced to 12,355 unique intensities (5.0 to 1.65 Å) with an *R*-merge of 4.3% for all data to a resolution of 1.65 Å (78.8% complete) using the XDS software package (16) (see Table I).

Met Cobalt Myoglobin—The unit cell dimensions were $a = 64.53$ Å, $b = 30.96$ Å, $c = 34.89$ Å, and $\beta = 105.8^\circ$. A total of 45,654 measured reflections from 120 images ($\Delta\omega = 1.5^\circ$) were reduced to 11,644 unique intensities (5.0 to 1.65 Å) with an *R*-merge of 3.8% for all data to a resolution of 1.65 Å (74.5% complete) using the XDS software package (16) (see Table I).

Structure Refinement—The cobalt myoglobin structures were determined using starting coordinates for native sperm whale myoglobin (17) to calculate initial phases. Cycles of conventional positional refinement were carried out using X-PLOR (18, 19) alternated with manual fitting using the CHAIN software package. The crystal structures were all refined with Engh and Huber topology and parameter files (20) for the protein and TIPS3P topology and parameter files for the solvent. Our own topology and parameter files were used for the refinement of the heme unit (based upon Kuriyan's) with no metal-nitrogen restraints or energies on the cobalt atom to remove any bias in the metal position. The crystallographic refinements converged to *R*-factors of 18.1, 16.2, and 16.4% for the deoxy, oxy, and met structures, respectively (see Table I).

Data Analysis—The error in the position of the light scattering atoms

in these cobalt myoglobins can be estimated from a Luzzatti plot to be about 0.2 Å. The metal, a heavy scatterer, is even further pinpointed by the 24 atoms making the plane of the porphyrin ring, rendering a positional error of about 0.04 Å. The standard deviation in the position of the metal atom in cobalt myoglobins can also be estimated to be 0.02 Å based upon SHELXL least squares refinement.

The method of Kabsch (21) was used to superpose atomic coordinates by overlaying the α carbons of the protein or the aromatic carbons of the heme. The program RIBBONS and was used to display the results.

RESULTS AND DISCUSSION

The aquomet form of cobaltic myoglobin was crystallized using the same protocol as that for native sperm whale myoglobin. Preparation of the samples for the deoxy form of cobaltous myoglobin required several attempts. Freshly reconstituted cobalt(II) myoglobin was first set up for crystallization in its deoxy form in an anaerobic glove box to prevent oxidation to the aquomet cobalt(III) form of the protein. However, no crystals grew in this deoxy state; all crystals grown (starting after a period of six to eight months following setup) and then mounted in the glove box turned out to be the oxidized form of the protein as determined by the presence of a sixth coordinated ligand in electron density maps. The crystalline deoxy state was achieved only by reducing an oxidized cobalt myoglobin crystal overnight and mounting it in the absence of dioxygen. The oxy form of cobalt myoglobin was attained by bubbling pure dioxygen through a mother liquor solution containing a crystal of previously reduced cobalt deoxymyoglobin immediately prior to data collection.

In general, the structures of cobalt myoglobin are analogous to those of their native iron-containing counterparts. The structures of the oxidized forms are very similar with water coordinated to both iron(III) and cobalt(III) at the sixth coordination site (see Table II). Iron lies -0.22 Å out of the porphyrin plane toward the proximal side and 2.17 Å from the N $_{\epsilon}$ of the histidine 93. Cobalt lies -0.11 Å out of the porphyrin plane and 2.06 Å from the proximal histidine. The shorter cobalt-histidine 93 bond distance corresponds to the cobalt-methyl imidazole bond distance of 1.94 Å in a model cobalt(III) porphyrin compound (22). The hydrogen bonding distance of 2.87 Å between N $_{\epsilon}$ of distal histidine 64 and the coordinated water in cobaltic myoglobin is only slightly larger than the distance observed in ferric myoglobin (2.65 Å).

The dioxygen ligand in cobalt oxymyoglobin is arranged in much the same geometry as that found in native sperm whale oxymyoglobin (23). The metal-O1-O2 angle is 8° smaller in the case of cobalt substitution (Table II), just outside the error limit of 5°. There is a small difference in the position of distal histidine 64 between the native and cobalt proteins (see Fig. 1). In iron-containing native oxymyoglobin, terminal oxygen atom O2 lies closer to N $_{\epsilon}$ of the distal histidine (2.77 Å) than metal-bound oxygen atom O1 (2.95 Å). In cobalt oxymyoglobin, the histidine N $_{\epsilon}$ to O2 distance is 3.01 Å versus 2.72 Å for the histidine N $_{\epsilon}$ to O1 distance. The electron density and the thermal parameter for O2 in the present cobalt oxymyoglobin structure are as well defined as those for O1. Hydrogen bonding to either oxygen atom in cobalt oxymyoglobin is consistent with previous conclusions derived from the EPR and resonance Raman studies (3–6, 24). Unpaired electron spin density appears to be distributed almost equally between the two oxygen atoms and there are strong couplings between the porphyrin and the bound oxygen vibrations. A structure of cobalt oxymyoglobin at 1.5-Å resolution was reported previously (13) and, although the refinement was incomplete, the cobalt-ligand geometry and the hydrogen bond distance between distal histidine N $_{\epsilon}$ and O1 of the ligand (2.88 Å) are very similar to those presented here.

The main differences between the oxy and deoxy structures of native iron-containing sperm whale myoglobin (F_{obs} oxy –

TABLE II
Selected myoglobin bond lengths and angles from crystallographic data

CoMb	PDB entry	Resolution	Co out-of-plane	Co-N (His93)	Co-Ligand	Ligand-Co-N(His93)	Co-O1-O2	CoOH...N (His64)
Deoxy	1 YOG	1.65 Å	-0.15 Å	2.18 Å				
Oxy	1 YOI	1.65	-0.09	2.08	2.03 Å	171°	109°	
Oxidized	1 YOJ	1.65	-0.11	2.06	2.19	176		2.87 Å
FeMb	PDB entry	Resolution	Fe out-of-plane	Fe-N (His93)	Fe-Ligand	Ligand-Fe-N(His93)	Fe-O1-O2	FeOH...N (His64)
Deoxy	1MBD	1.40 Å	-0.35 Å	2.10 Å				
Deoxy	5MBN	2.00	-0.38	2.17				
Oxy	1MBO	1.60	-0.19	2.07	1.83 Å	174°	116°	
Met	4MBN	2.00	-0.22	2.17	2.10	175		2.65 Å
Deoxy ^a	1VXG	1.70	-0.26	2.31				
Met ^a	1VXH	1.70	-0.13	2.15	2.17	176		2.72
Deoxy ^b	2MGL	2.00	-0.41	2.25				
Oxy ^b	2MGM	1.90	-0.14	2.19	1.94	174	118	
Met ^b	1MBW	1.90	-0.14	2.24	2.28	174		2.54
Met ^b	2MBW	1.50	-0.16	2.19	2.21	176		2.64

^a Crystals kept at pH 6, as reported by Yang and Phillips (17).

^b Crystals grown in the P6 space group as reported by Quillin *et al.* (30).

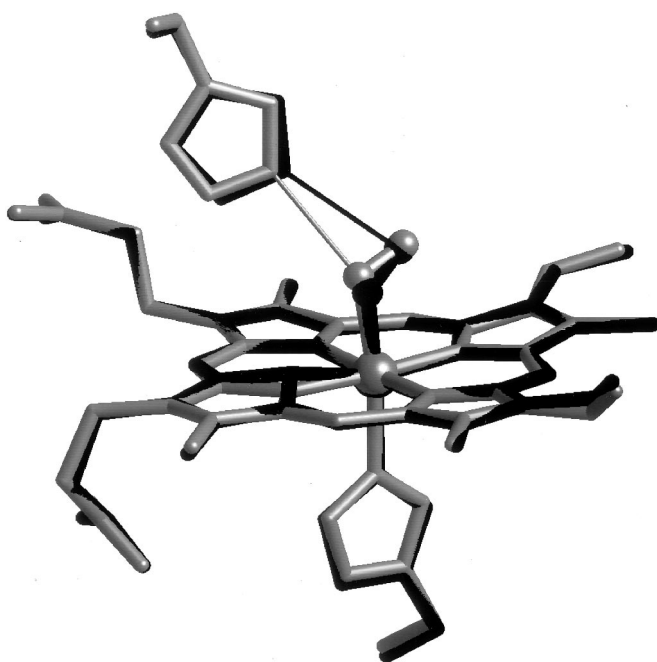


FIG. 1. Superposition of the native (1MBO, *black*) and cobalt (1YOI, *gray*) oxymyoglobins displaying the difference in hydrogen bonding from distal histidine 64 to the dioxygen ligand. Of each holoprotein, only the metalloporphyrin, the dioxygen ligand, and histidine residues 64 and 93 are shown. Hydrogen bonds are represented by *thin lines*.

F_{obs} deoxy) are a sideways movement of the heme upon loss of the dioxygen ligand, manifesting as electron density around the metal in the plane of the porphyrin, and the loss of the coordinated met water and the distal histidine-bound sulfate. This is also the case in cobalt-substituted myoglobin (see Fig. 2).

The most significant difference between the structure of cobalt deoxymyoglobin and that of native sperm whale deoxymyoglobin is the position of the metal atom with respect to the protoporphyrin plane. The iron(II) atom in native oxymyoglobin (space group $P2_1$) has an initial displacement of -0.19 Å from the plane of the porphyrin ring and then moves an additional -0.16 Å upon deoxygenation (Table II). This movement is larger in the more open P6 space group of recombinant myoglobins, which may better reflect the environment of the fully solvated protein (25). The cobalt(II) atom in reconstituted myoglobin (Fig. 2), refined without any bias on metal position, also shows movement in the same direction out of the porphy-

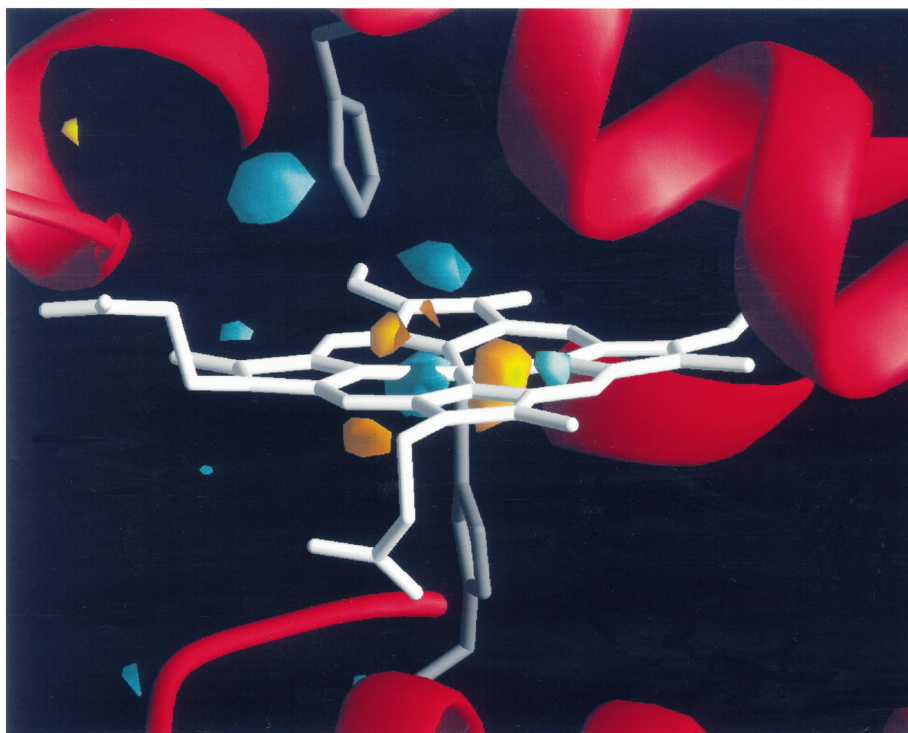
rin plane as well, but to a much lesser degree: only -0.06 Å starting from a smaller initial displacement in the oxy form. The cobalt-proximal histidine 93 bond distance of 2.18 Å in the deoxy structure corresponds to the cobalt-methyl imidazole bond distance of 2.16 Å in a model cobalt(II) porphyrin compound (26).

The difference in magnitude of metal movement between the native iron and reconstituted cobalt sperm whale myoglobins may be explained in terms of metal coordination geometry and spin state. The iron in the native myoglobin moves from 5-coordinate high spin ($S = 2$) to 6-coordinate low spin ($S = 0$) upon oxygenation of the ferrous protein. The cobalt metal also makes the 5- to 6-coordinate shift upon ligand binding, but with no change in spin state ($S = 1/2$). If spin state alone contributes to metal movement relative to the porphyrin plane, no cobalt movement would be expected (8). The results in Table II suggest that both factors contribute to the displacement of the metal out the heme plane on losing the dioxygen ligand. Cobalt moves out of the porphyrin plane upon deoxygenation, albeit to a lesser extent than iron, showing that change in coordination geometry alone can affect the metal position.

The movement of iron into and out of the porphyrin plane has been cited as a driving force in the mechanism of cooperative oxygen binding in the human hemoglobin tetramer (8, 27). Cooperativity is diminished in human hemoglobin when the iron is replaced with cobalt; the Hill coefficient decreases from 2.8 to 2.2 (1, 14). The free energy change associated with cooperativity in cobalt hemoglobin is one-half to one-third that in native hemoglobin (28). The structure of human cobalt deoxyhemoglobin has been refined to 2.5 -Å resolution (29). The cobalt atom was found to lie 0.33 Å out of the porphyrin plane as opposed to 0.56 Å for the iron in native hemoglobin. In deoxymyoglobin cobalt is displaced 0.15 Å out of the plane of the porphyrin, whereas the iron displacement is ~ 0.35 Å. The 0.20 -Å difference between the cobalt and iron positions in deoxymyoglobins is similar to that seen for the corresponding deoxyhemoglobins (0.23 Å). The smaller overall movement of the metal during ligand binding explains the partial loss of cooperativity in cobalt hemoglobin when compared to the native iron-containing protein.

Two views have been put forward to explain the multiphasic kinetics of picosecond geminate ligand rebinding to native sperm whale myoglobin. The first attributes the slowing of the reaction to the movement of the iron atom out of the plane of the porphyrin and away from the free ligand upon dissociation (9). The second view (10) states that variability in the structure of the distal pocket cause ligands to distribute differently as they diffuse away from the metal atom. In simulations of metal

FIG. 2. Difference map of cobalt myoglobins in the vicinity of the ligand binding site (coefficients $F_{\text{obs}} \text{ aquomet} - F_{\text{obs}} \text{ deoxy}$ at 4.5). The deoxyprotein shown is colored red with its cobalt protoporphyrin IX white. Cyan features denote electron density in the metmyoglobin structure not found in deoxymyoglobin, whereas gold features denote density found only in the deoxymyoglobin structure. This difference density reveals that the metal-coordinated met water and a distal histidine-bound sulfate are not present in cobalt deoxymyoglobin and indicates that the small displacement of cobalt in the deoxy state is coupled with a large sideways metalloporphyrin movement.



movements in iron-containing mutants (11, 30), no significant correlation between iron positions and geminate rates was seen. Cobalt myoglobin also shows multiphasic geminate ligand rebinding reactions which are similar to those observed for native iron myoglobin (10). The analogous trend in geminate rebinding rates among mutant proteins with both iron and cobalt supports the view that ligand movement in the distal pocket is the primary determinant of the multiple phases seen for geminate recombination on time scales greater than ~ 30 ps. On shorter time scales, the dioxygen-metal bond formation reaction is much faster for cobalt than for iron-containing myoglobins due to the greater intrinsic reactivity of the cobaltous ion (conservation of spin momentum, Ref. 31) and its closer proximity to the plane of the porphyrin ring.

Acknowledgments—We thank Fan Yang for help in the crystallization of cobalt metmyoglobin. Michael Soltis and Michael Stowell at the Stanford Synchrotron Radiation Laboratory collected the 1.5 Å data on wild-type metmyoglobin (2MBW) and their work was supported by the Department of Energy and the National Institutes of Health (rotation camera facilities).

REFERENCES

- Hoffman, B. M., and Petering, D. H. (1970) *Proc. Natl. Acad. Sci. U. S. A.* **67**, 627–643
- Chien, J. C. W., and Dickinson, L. C. (1972) *Proc. Natl. Acad. Sci. U. S. A.* **60**, 2783–2787
- Yonetani, T., Yamamoto, H., and Iizuka, T. (1974) *J. Biol. Chem.* **249**, 2168–2174
- Ikeda-Saito, M., Iizuka, T., Yamamoto, H., Kayne, F. J., and Yonetani, T. (1977) *J. Biol. Chem.* **252**, 4882–4887
- Kitagawa, T., Ondrias, M. R., Rousseau, D. L., Ikeda-Saito, M., and Yonetani, T. (1982) *Nature* **298**, 869–871
- Ikeda-Saito, M., Lutz, R. S., Shelly, D. A., McKelvey, E. J., Mattera, R., and Hori, H. (1991) *J. Biol. Chem.* **266**, 23641–23647
- Lee, C. H., Peisach, J., Dou, Y., and Ikeda-Saito, M. (1994) *Biochemistry* **33**, 7609–7618
- Hoffman, B. M., Spilburg, C. A., and Petering, D. H. (1971) *Cold Spring Harbor Symp. Quant. Biol.* **36**, 343–348
- Petrich, J. W., Lambry, J.-C., Kuczera, K., Karplus, M., Poyart, C., and Martin, J.-L. (1991) *Biochemistry* **30**, 3975–3987
- Ikeda-Saito, M., Dou, Y., Yonetani, T., Olson, J. S., Li, T., Regan, R., and Gibson, Q. H. (1993) *J. Biol. Chem.* **268**, 6855–6857
- Quillin, M. L., Li, T., Olson, J. S., Phillips, G. N., Jr., Dou, Y., Ikeda-Saito, M., Regan, R., Carlson, M., Gibson, Q. H., Li, H., and Elber, R. (1995) *J. Mol. Biol.* **245**, 416–436
- Padlan, E. A., Eaton, W. A., and Yonetani, T. (1975) *J. Biol. Chem.* **250**, 7069–7073
- Petsko, G. A., Rose, D., Tsernoglou, D., Ikeda-Saito, M., and Yonetani, T. (1978) in *Frontiers of Biological Energetics, From Electrons to Tissues* (Dutton, P. L., Leigh, J. S., Jr., and Scarpa, A., eds) pp. 1011–1016, Academic Press, New York
- Yonetani, T., Yamamoto, H., and Woodrow, G. V., III (1974) *J. Biol. Chem.* **249**, 682–690
- Kendrew, J. C., Dickerson, R. E., Strandberg, B. E., Hart, R. G., Davies, D. R., Phillips, D. C., and Shore, V. C. (1960) *Nature* **185**, 422–427
- Kabsch, W. (1993) *J. Appl. Cryst.* **26**, 795–800
- Yang, F., and Phillips, G. N., Jr. (1996) *J. Mol. Biol.* **256**, 762–774
- Brünger, A. T., Kuriyan, J., and Karplus, M. (1987) *Science* **235**, 458–460
- Brünger, A. T. (1992) *X-PLOR Version 3.0 Manual*, Yale University
- Engh, R. A., and Huber, R. (1991) *Acta Cryst. Sect. A* **47**, 392–400
- Kabsch, W. (1978) *Acta Cryst. Sect. A* **34**, 827–828
- Bang, H., Edwards, J. D., Kim, J., Lawler, R. G., Reynolds, K., Ryan, W. J., and Sweigart, D. A. (1992) *J. Am. Chem. Soc.* **114**, 2843–2852
- Phillips, S. E. V. (1980) *J. Mol. Biol.* **142**, 531–554
- Dickinson, L. C., and Chien, J. C. W. (1980) *Proc. Natl. Acad. Sci. U. S. A.* **77**, 1235–1239
- Phillips, G. N., Jr. (1989) *Biophys. J.* **57**, 381–383
- Scheidt, W. R. (1974) *J. Am. Chem. Soc.* **96**, 90–94
- Perutz, M. F. (1970) *Nature* **288**, 726–734
- Imai, K., Yonetani, T., and Ikeda-Saito, M. (1977) *J. Mol. Biol.* **109**, 83–97
- Fermi, G., Perutz, M. F., Dickinson, L. C., and Chien, J. C. W. (1982) *J. Mol. Biol.* **155**, 495–505
- Quillin, M. L., Li, T., Olson, J. S., and Phillips, G. N., Jr. (1993) *J. Mol. Biol.* **234**, 140–155
- Frauenfelder, H., and Wolynes, P. G. (1985) *Science* **229**, 337–345